Journal of Structural Geology, Vol. 10, No. 1, pp. 41 to 52, 1988
Printed in Great Britain

0191-8141/88 $03.00 + 0.00
Pergamon Press plc

Symmetry of pebble-deformation involving solution pits and slip-lineations in the northern Alpine Molasse Basin

FRANK SCHRADER

Geologisches Institut der Universität, Nußallee 8, D-53 Bonn 1, F.R.G.

(*Received* 24 *July* 1986; *accepted in revised form* 14 *July* 1987)

Abstract—Deformation features on pebbles of the Alpine Molasse Basin are most clearly developed in carbonate components. Ductile distortion is small; most of the pebbles moved against each other to produce solution pits and slip-lineations on the pebble surfaces. The complete lineation field has a triaxial geometry. From a compressional *axis of divergence* with maximum solution, fields of diverging lineations extend to meet at a *plane of convergence*. Their ends bend away from an *intermediate axis* towards an (extensional) *axis of convergence*. The strain-symmetry is pure shear for orthogonal lineation-field axes, uniaxial compression and extension representing special cases. The angle α between the divergent and the convergent axes decreases from 90 to 0° with the transition from pure to simple shear. For Molasse pebbles α angles between 90 and 60° were usually observed. Regional compression developed perpendicular to the Alpine structures and parallel to bedding, with increasing deviations near the Alpine border. Zones are recorded of vertical and horizontal extension and of compression perpendicular to bedding and horizontal extension perpendicular to the Rhinegraben existing at the northern border of the Molasse Basin.

Kurzfassung—Molassegerölle sind von Lösungsgruben und damit verbundenen Gleitlineationen deformiert worden, am deutlichsten die karbonatischen Komponenten. Die plastische Verformung ist gering, die meisten Gerölle bewegten sich reibend als starre Körper gegeneinander. Der Versetzungssinn der Bewegungen ist durch Unterscheidung einengender und dehnender Lineationen erkennbar. Das vollständige Lineationsfeld hat eine dreiachsige Geometrie. Von einer eingeengten *Divergenzachse* mit maximaler Anlösung streben zwei halbkreisförmige Lineationsfeldteile fort und treffen sich an der *Konvergenzebene*. Dort biegen ihre Enden von einer *intermediären Achse* fort und laufen auf eine gedehnte *Konvergenzachse* zu. Im Falle orthogonaler Lineationsfeldachsen ist die Verformungs-Symmetrie zweischarige Zerscherung, Spezialfälle sind einachsige Einengung und einachsige Dehnung. Der Winkel α zwischen Einengungs- und Dehnungsrichtung nimmt ab mit dem Übergang von zweischariger (90°) zu einschariger (0°) Zerscherung. Normalerweise liegen die Winkel an Molassegeröllen zwischen 90 und 60°. Die regionale Einengungsrichtung verläuft senkrecht zu den alpinen Strukturen und parallel zur Schichtungsebene; Abweichungen nehmen gegen den Alpenrand hin zu. Zonen horizontaler oder vertikaler Dehnung können aufgenommen werden. Am Molassenordrand existiert Einengung senkrecht zur Schichtungsebene und horizontale Dehnung senkrecht zum Rheintalgraben.

INTRODUCTION

IN THE Tertiary conglomerates ('Nagelfluh') of the northern Alpine Molasse Basin (Fig. 1), adjacent pebbles indent each other forming contact-pits (Trurnit 1968). These phenomena have been known for a long time (Blum 1840) and their origin attributed to various physical or chemical changes during diagenetic or tectonic processes. A mechanism of pressure solution induced by tectonic forces is now generally favoured (Behrens & Wurster 1972).

Molasse rocks have been subjected only to diagenesis with little coalification (Teichmüller & Teichmüller 1975, Kübler *et al.* 1979). Cementation has produced harder clays, sandstones and conglomerates (Breddin 1964) only in the early strata of Oligo-Miocene age, close to the Alpine border, which were buried deeply; the principal cement is calcite (Füchtbauer 1964).

Pelites or psammites were shortened by up to 25%, as indicated by thin-shelled fossils (Voll 1953, Breddin 1964, Albrecht & Furtak 1965), producing cleavage in places. In the conglomerates cleavage is rarely developed, but a small amount of material from pebbles is removed by solution at their contacts with some crushing, particularly of phyllosilicate pebbles. In pebbles without crushing, seldom has more than a small percentage of their volume been removed at solution-contacts, and the opened (and authigenically filled) space between extended pebbles is even less. A small amount of compaction results in the conglomerates, caused by more compression in the pits than extension between the pebbles. Overall the pebble deformation is regarded as isovolumetric, although increasing compaction of the entire Molasse sediments towards the Alpine border can be deduced from the velocities of elastic waves (Lohr 1969).

In tectonics, plastically deformed pebbles are often used to determine the shape of the strain ellipsoid (Flinn 1956, Hossack 1968, Lisle 1979, Greiling 1985). In such studies it is generally assumed that the pebbles are deformed with a similar ductility to their matrix. Molasse pebbles, however, mainly reacted as rigid bodies, which moved against each other producing indentation and lineations. These features provide insight into the relative displacements of the pebbles and their matrix which may be utilized in a structural analysis of the basin.

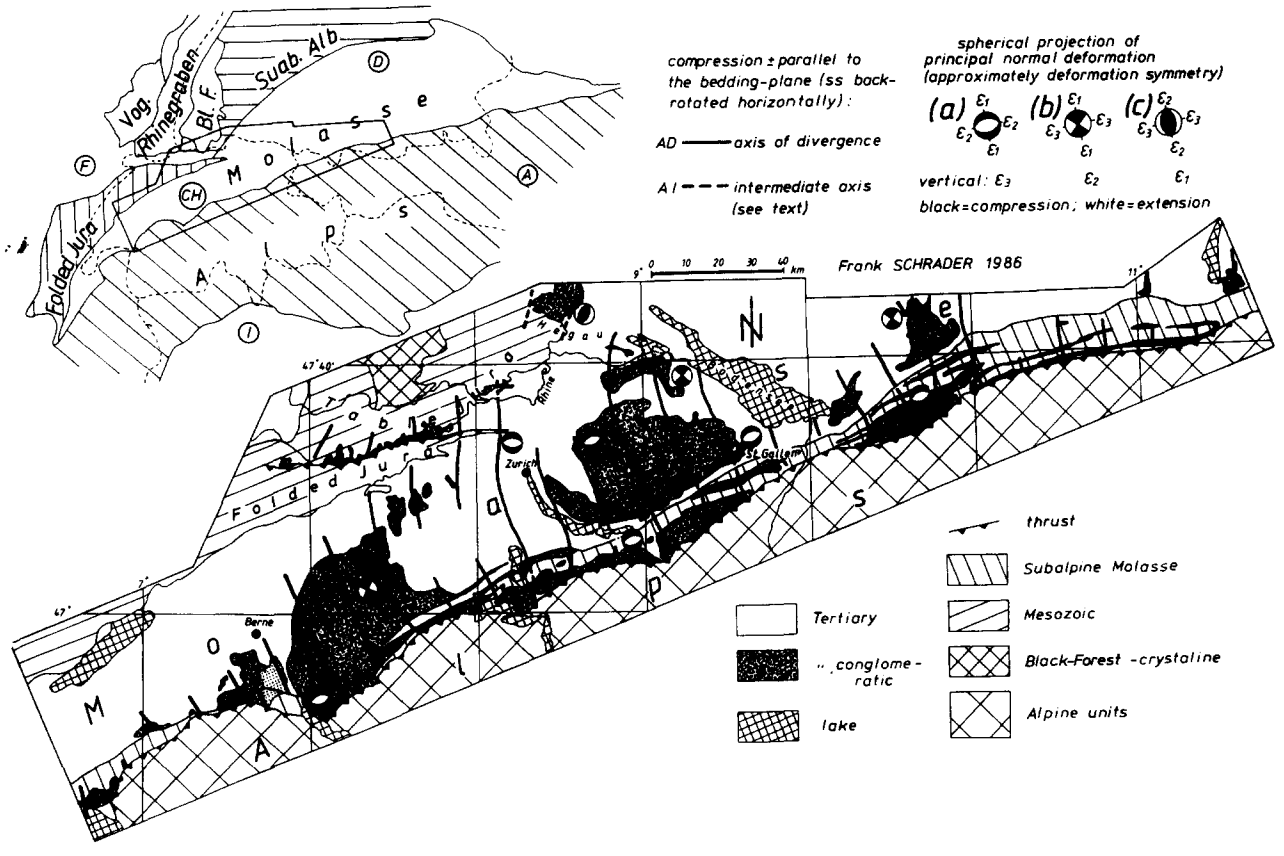

Fig. 1. Pebble deformation in the western Molasse Basin. Horizontal compression (axis of divergence, AD, parallel to bedding) is directed perpendicular to the Alpine structures and the eastern folded Jura extension either vertical (a) or horizontal (b) parallel to them. In the north (Hegau area), compression is vertical and extension horizontal perpendicular to the Rhinegraben. The intermediate axis (AI) as the horizontal component of compression is parallel to the Rhinegraben (c).

DEFORMATIONAL FEATURES

The pebbles are indented superficially by their less soluble neighbours producing contact pits, which are most striking when exposed on weathered surfaces. Indentation can be perpendicular to the surface (Fig. 2a) or oblique (Fig. 2g & h). Most of the pits have been excavated by pressure solution with little mechanical rupture. Large, well preserved pits show an area with vertical indentation columns surrounded by an area with oblique columns. These change to slip-lineations on the pebble surface around the pits (Fig. 2g & h). These lineations can be arrangements of small, oblique pits (stylolitic lineation of adjacent sand-grains, Fig. 2f up), grooves (frictional wear striations, parallel to the pebble surface, Fig. 2f down) or fibrous syntaxial mineral growths (Fig. 2e). They are most clearly developed on smooth pebble surfaces and are pervasive in the whole unweathered rocks.

Pits and lineations cover the entire pebble surface; pits being produced by bigger neighbours and lineations by smaller particles of the matrix. Together they show the movements of adjacent particles relative to the pebble. Areas of penetrating motion gradually change to areas of extending motion. Gaps and stylolites in pebbles are less frequent. Heim (1919) tried to separate 'solution' pits and 'dislocated' slip-lineations (because pits are broken by dislocations he thought their ages to be different). Now, both are thought to be (nearly) contemporaneous. Pebbles indented mutually by producing pits or, when pressure-solution was not able to relieve the stress at the contacts (McEwen 1981) fast enough, the pebble fractured and gaps formed (Fig. 2h). Usually, the conglomerates consist of high percentages of carbonate pebbles and pressure solution has affected mainly these components. Most of the crystalline and quartzite components were only deformed where they touched mutually; in their deformation, gaps play a more important role.

Deformation field

If the lineations are conserved all over the pebble surface, the complete field of deformational displacements can be deduced and in the general case, this has a triaxial geometry (Fig. 3). From an *axis of divergence* between two centrifugal poles (Schrader 1987) with maximum solution and perpendicular pitting (Fig. 2a), two lineation fields extend and meet with decreasing solution at the *plane of convergence* (Fig. 2b). Their ends bend away from an *intermediate axis* (between two spreading points, Fig. 2c) towards an *axis of convergence* (between two aiming points, Fig. 2d) where calcite is sometimes deposited. Thus, for any pebble the linea-

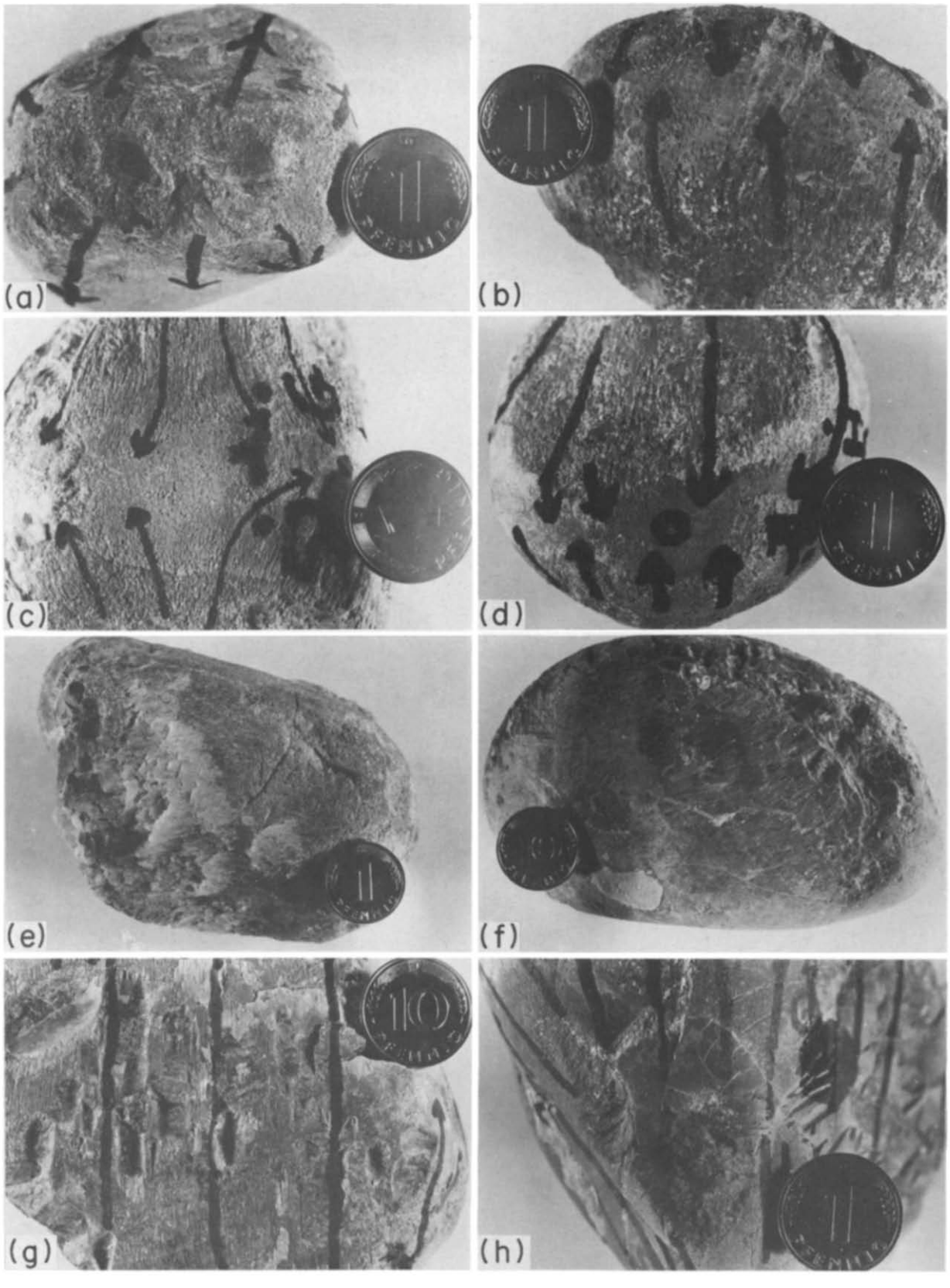

Fig. 2. Deformational features of Molasse pebbles. (a) Axis of divergence showing the lineations extend from the solution pits perpendicular to the image plane. (b) Plane of convergence where two lineation fields are directed against each other; the incision depth of solution striation decreases towards the plane. (c) Spreading point (intermediate axis): at the plane of convergence both lineation fields spread oppositely. (d) Axis of convergence where the lineations converge and the solution of the pebble surface reaches a minimum on the plane of convergence. (e) Crystal fibre slip-lineation (motion of the matrix right to left) with steps and idiomorphic crystals pointing towards the slip-direction. (f) Solution (right) to parallel (middle) lineation produced by matrix motion from right to left; the steep sides of the carvings point against the slip-direction, their depth decreases towards the middle of the pebble. (g) At the rear of oblique impressions (particularly top left) authigenic calcite is redeposited behind the indenting pebble (motion bottom towards top). (h) Bulge in front of an impression oblique to the pebble surface (matrix-motion bottom towards top).

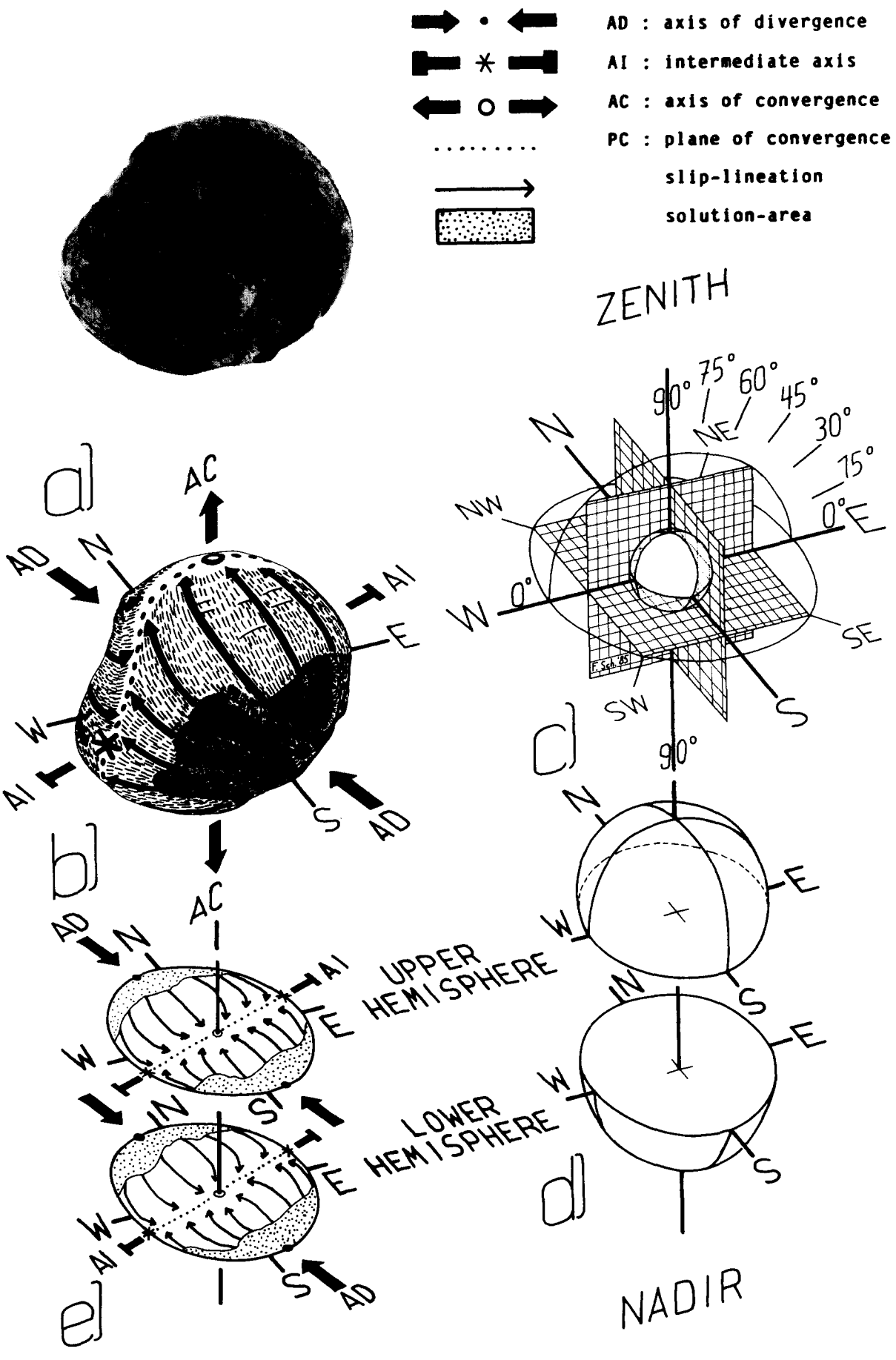

Fig. 3. Deformation field of Molasse pebbles. (a) and (b) From an *axis of divergence* (AD) with maximum solution, two circular striation fields are directed against each other and meet at the *plane of convergence*. Their ends bend away from an *intermediate axis* (AI) between two spreading points towards an *axis of convergence* (AC). (c) System of spherical co-ordinates for pebble measurement. (d) For description of its surface data both hemispheres are necessary and can be represented on two Schmidt equal-area nets (e). For further explanations see text.

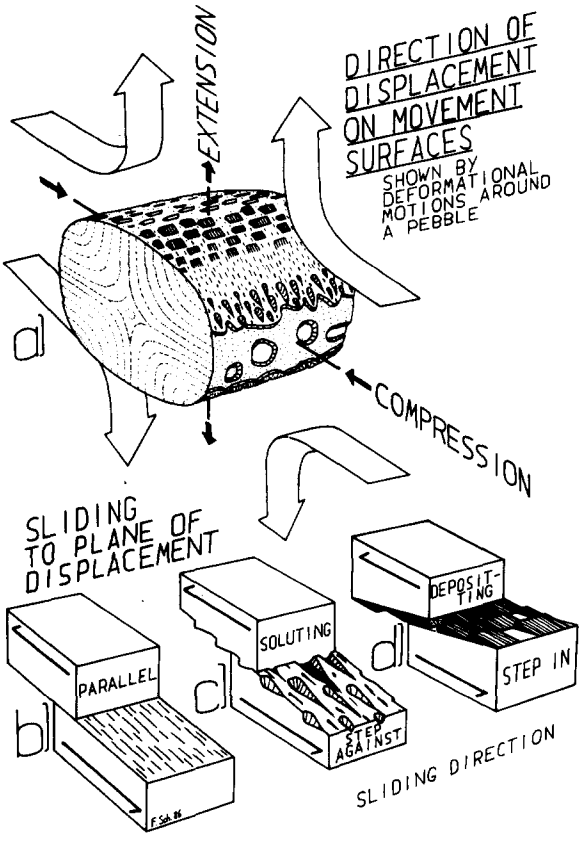

Fig. 4. Sense of displacement on pebble surfaces. (a) The motion-lineations penetrate vertically into the pebble surface in the direction of compression, but farther away the angles decrease and a solution striation notches the pebble with carvings against the direction of displacement. The angles become parallel to the pebble surface and increase towards the direction of extension with crystal fibre growth lineations, whose steps point into the direction of the motion. (b) Motion parallel to the movement surface generates longitudinal grooves. (c) Compressive motion with solution-carvings with the steep side directing against the motion. (d) Extending motion (deposited crystal fibres) with steps in the direction of displacement.

tions and pits define three axes in the field of particle motion: an axis of divergence (AD) which is the direction of compression, an axis of convergence (AC) which is the direction of maximum extension and an intermediate axis (AI).

The bipolar lineation field between the centrifugal poles (lineation divergence) was recorded by Behrens & Wurster (1972) in the Bavarian Subalpine Molasse. Similar poles were found by Campredon *et al.* (1977) in the Subalpine Ranges in southeastern France ("pôles de compression") and by Estevez & Sanz de Galdeano (1983) in the Betic Ranges in southern Spain ("pressure-solution poles"). Sanz de Galdeano & Estevez (1981) also show a figure with converging lineations, perhaps corresponding to the aiming points. Ferrandini & Petit (1982) and Petit *et al.* (1985) found a different symmetry of lineations on pebble surfaces from the High Atlas Range in Morocco.

Displacement sense of lineations

To complete the description of the displacement fields it is necessary to know the sense of displacement on the pebble surface. Whether the step on a fault surface points in the direction of the motion (congruous, Hancock 1985), or in the opposite sense (incongruous) can be decided by distinguishing compressional and extensional lineations on pebble surfaces, similar to those in massive carbonate rocks according to Arthaud & Mattauer (1969) and Mattauer (1980). There are three types of lineation with gradual transitions (Fig. 4a).

(1) Solution striation with pits indenting in the direction of compression or somewhat oblique carvings whose steep side is directed opposite (incongruous) to the direction of the motion (Figs. 2f and 4c). The bigger pits sometimes show a bulge in front of the indenting neighbour (Fig. 2h) or the deposition of calcite at the rear of the pit, where the neighbour moved away during further indentation (Fig. 2g).

(2) Sliding parallel to the pebble surface with longitudinal grooves or fibres (Figs. 2f and 4b).

(3) Mineral fibres deposited in the direction of extension with steps whose steep side points in the direction of the motion (Figs. 2e and 4d).

Measurement

For measurement (Behrens & Wurster 1972, Behrens 1977) the pebble is put into a system of spatial polar co-ordinates in its *in situ* orientation (Fig. 3c). The origin of the co-ordinates is the center of gravity of the pebble. All features on the pebble surface are measured in spherical angles between the cardinal points and the horizontal plane; their distances from the pebble's center, i.e. the pebble's shape, are neglected. On nearly spherical pebbles the deviations are small. Surface features are recorded on a Schmidt equal-area net and thus can be combined easily for several pebbles. To represent both hemispheres two nets are necessary. The lineations marked by course-lines on the pebble surface are represented by lines, and the pits by areas of solution in the projection. The axes of the displacement field become points in the spherical projection and only one net is necessary for their representation.

STRAIN SYMMETRY

A clear, triaxial deformation field shows the strain-symmetry of a single deformation phase. Sometimes there are rather confusing arrangements of lineations on a pebble surface. In most cases it is possible to assign the lineations to different, triaxial systems, originating in different deformational phases.

The slip-lineations demonstrate motions during the deformation of the conglomerates. Fields of particle paths have been calculated by Hoeppener (1964), Ramberg (1975), Ramsay & Huber (1983) or imitated experimentally by Hoeppener *et al.* (1983). Their shape depends on the deformation symmetry and there are different arrangements for pure shear, simple shear and closed motions of the particles. The location of the origin of the reference frame is assumed fixed in the

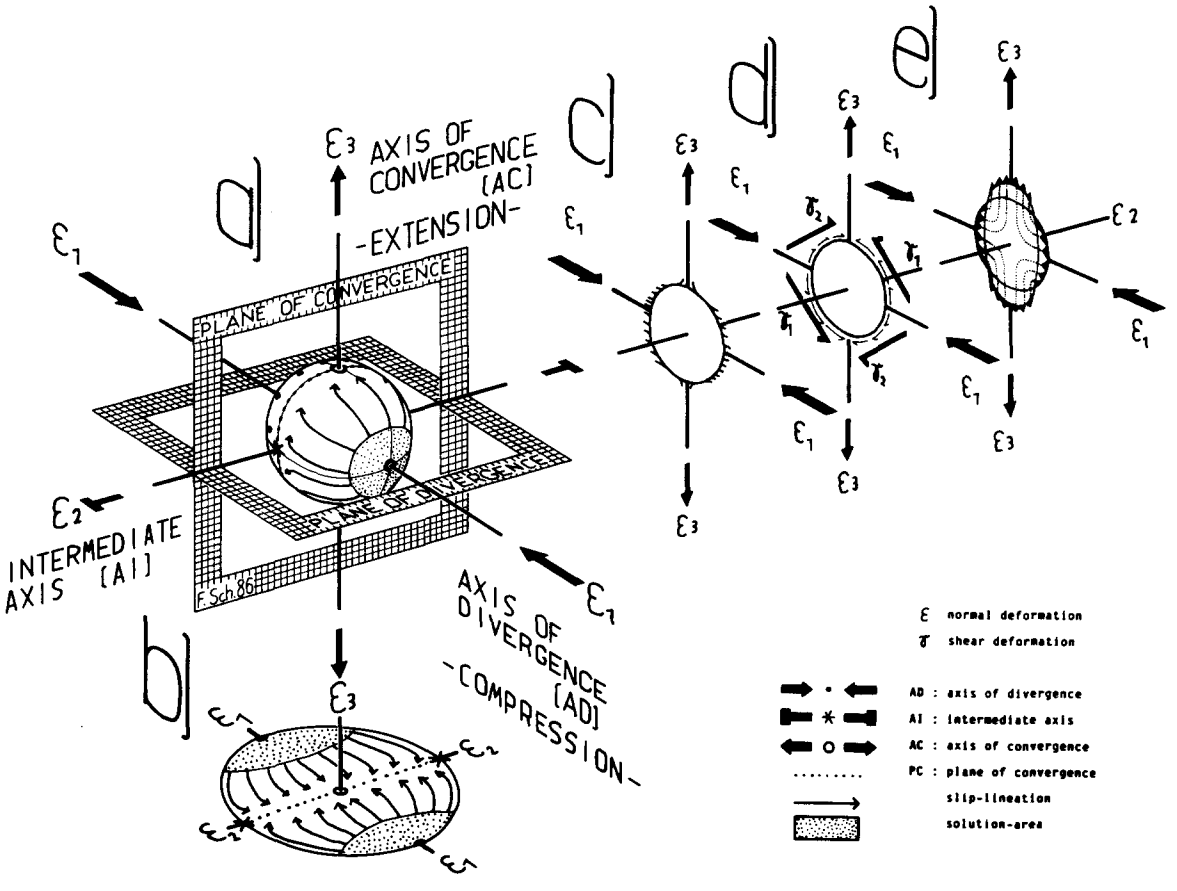

Fig. 5. Orthorhombic deformation field (pure shear). (a) AD, AI and AC are orthogonal and coincide with the principal normal deformations $\varepsilon_{1,2,3}$. (b) Between AD and AC the halves of the lineation field are equal. (c) Around soluble pebbles, the angles between the surface and compressive (parallel to ε_1) or extending (parallel to ε_3) motion-lineations are nearly 90° and correspond to the ideal particle paths of isotropic deformation. (d) Around less soluble (quartz-) pebbles, the lineations are deflected towards a position more parallel to the pebble surface. Between ε_1 and ε_3 are two symmetric principal shear-deformations $\gamma_1 = \gamma_2$. (e) The sum of ε and γ produces the field of particle motions along orthogonal hyperbolas.

deformed body and moves with deformation, i.e. the described motions can be seen by an observer located in the origin of the reference frame and particle motions are regarded relative to it. Thus the system shows the motions of particles relative to each other from the direction of compression towards the direction of extension.

Theoretical particle paths are calculated for an ideal isotropic, homogenously deformed body. The most soluble pebbles (marls) show the ideal configuration: perpendicular penetration around the divergence axes, nearly perpendicular grown fibres (or idiomorphic crystals) around the convergence axes (Fig. 5c). The lineations on less soluble components (quartz) are nearly parallel to the pebble surfaces (Fig. 5d), into which solution could not penetrate. Thus adjacent pebbles interact with one another and the angles of motion between axes and pebble surfaces around insoluble pebbles differ from the ideal paths in a homogenously deformed body. The differences are eliminated in the spherical projections, where lineations are represented as if they were parallel to the plane on which they occur.

The particle motions take place in a constant way throughout the deformation process, and thus the problem needs no incremental approach. The paths are in general hyperbolas (Fig. 6b), and at every point their tangents can be analysed into a radial component ε and a tangential component γ (Hoeppener *et al.* 1983) (Fig. 6a). Only the tangents of the intersecting parts of the particle paths are visible on the pebble surfaces and they are deflected towards a position more or less parallel to the pebble surface, depending on the solubility.

The ellipsoid of the radial (normal) component of the infinitesimal particle motions has principal directions $\varepsilon_{1,2,3}$ which should not be confused with the principal longitudinal strains ($X > Y > Z$) of the strain ellipsoid or the incremental strains $e_{i_{1,2,3}}$ (Ramsay & Huber 1983). The principal directions γ_1 and γ_2 are symmetrical at 45° between ε_1 and ε_3 (Fig. 6c), where the radial component ε is zero. The tangential component γ is equal to zero in the directions of the hyperbolas' asymptotes, which are the axes of the particle motion field. In the two-dimensional approach of Ramsay & Huber (1983), the asymptote a_1 corresponds to the axis of divergence and a_2 to the axis of convergence.

These axes are orthogonal, if γ_1 and γ_2 are of equal size; in this case of pure shear, they coincide with the axes X, Y, Z of the strain ellipsoid (finite longitudinal strains). Towards simple shear, γ_1 becomes larger than γ_2, and the directions where the resulting tangential motion γ is zero converge. Throughout the deformation process ε, γ and the axes of $\gamma = 0$ keep their position,

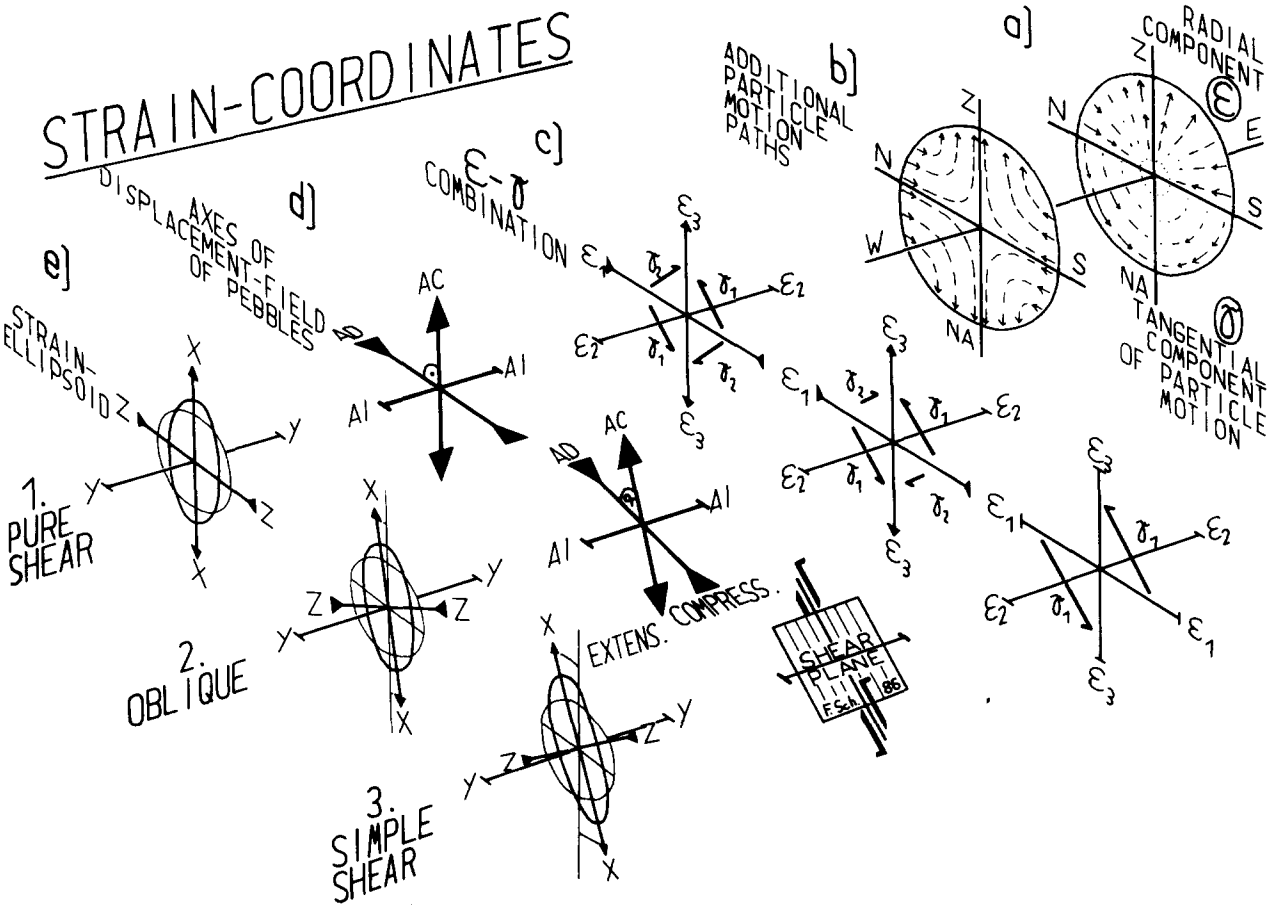

Fig. 6. Strain co-ordinates. The particle motions (b) are composed of a radial normal component ε (a, above) and a tangential shear component γ (a, below). (c) The ellipsoid $\varepsilon_1 > \varepsilon_2 > \varepsilon_3$ can be transformed to a monoclinic body by addition of two symmetrical, but unequal shears (pure shear for $\gamma_1 = \gamma_2$; oblique for $\gamma_1 > \gamma_2$; simple shear for γ_1; $\gamma_2 = 0$). (d) The axes of the lineation field (AD = axis of divergence, AI = intermediate axis, AC = axis of convergence) are the axes of the particle motion field. For pure shear $\alpha = 90°$, oblique $90° > \alpha > 0°$, simple shear $\alpha = 0$. (e) The orthogonal deformation ellipsoid ($X \geq Y \geq Z$) is the final result of deformation. For pure shear, X and Z are fixed during progressive deformation; for oblique shear, X rotates asymptotically towards the direction of extension; and for simple shear, X rotates asymptotically towards the plane of shear at 45° to ε_1 and ε_3.

whereas axes of the resulting finite-strain ellipsoid (X, Y, Z) rotate (Fig. 6e). X, the direction of maximum lengthening, asymptotically approaches the axis of convergence, with Z (shortening direction, unequal to the compressional axis of divergence) occupying a position perpendicular to X (Ramsay & Huber 1983, p. 232). In the case of pure shear (orthogonal strain directions), stress (Schmidt & Lindley 1938) and strain directions coincide (Hoeppener 1964).

Orthorhombic field

If the three axes of the lineation field are perpendicular to each other, this is the symmetry of pure shear (Sander 1948, Nadai 1950). The axis of divergence (AD) coincides with ε_1 and Z; the intermediate axis (AI) with ε_2 and Y, and the axis of convergence (AC) with ε_3 and X (Figs. 5a and 6e). $\gamma_{1,2}$ are of equal size (Figs. 5d and 6c), thus the particles in a plastically deformed sphere move along orthogonal hyperbolas (Fig. 5e). The parts of the lineation field are of equal length between AD and AC (Fig. 5b).

The orthorhombic field ($\varepsilon_1 > \varepsilon_2 > \varepsilon_3$) has two uniaxial special cases (Fig. 7a & b). If the intermediate and convergence axes are not differentiated into spreading and aiming points, then deformation is a uniaxial compression ($\varepsilon_1 > \varepsilon_2 = \varepsilon_3$). If divergence and intermediate axes are connected in a belt of solution the deformation is uniaxial extension ($\varepsilon_1 = \varepsilon_2 > \varepsilon_3$). As these axes coincide with the longitudinal strains X, Y, Z, the lineation field of particle motions is congruent to the strain ellipsoid.

Shape-induced scattering

Pebbles with exactly orthogonal lineation field axes are rare. An orthogonal strain produces orthogonal lineation fields only on spherical pebbles. Different shapes (ellipsoids or irregularities) distort the symmetry slightly, if the shape-axes and the directions of compression or extension do not coincide. In such cases, the lineation field's axes are transferred towards the edges. Maximum distortion occurs if a clear shape-plane of the pebble and the deformational directions include an angle of 45°. Around rigid inclusions in a less viscous matrix, the direction of the finite longitudinal strains will also deviate (Ghosh & Sengupta 1973). In an association of pebbles with differently oriented shape-planes, the

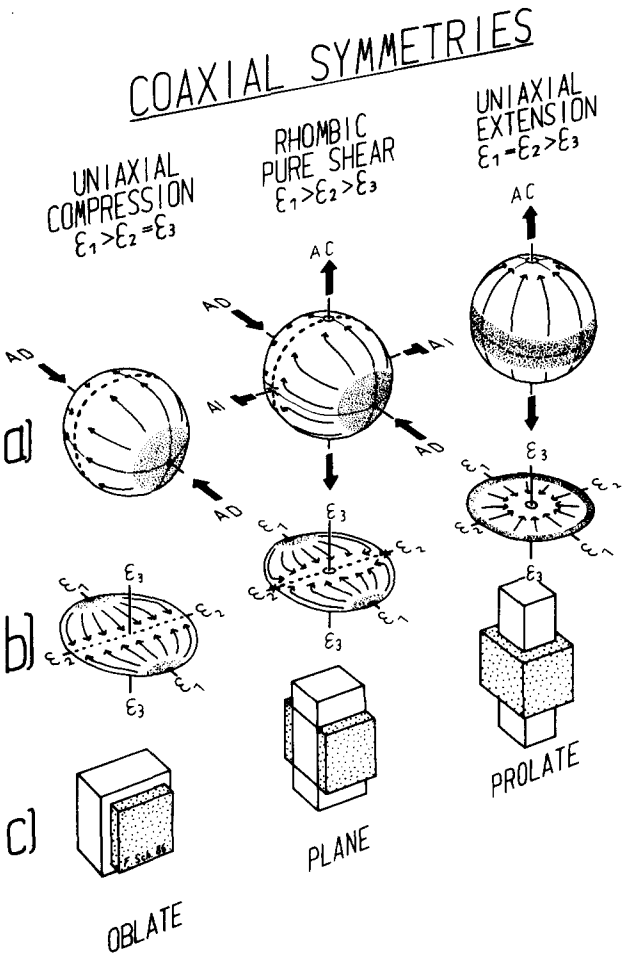

Fig. 7. Coaxial symmetries. (a) Lineation fields. Middle: the orthorhombic symmetry of orthogonal AD, AI and AC ($\varepsilon_1 > \varepsilon_2 > \varepsilon_3$) has two uniaxial special cases. Left: uniaxial compression ($\varepsilon_1 > \varepsilon_2 = \varepsilon_3$), where the plane of convergence is not differentiated into spreading and aiming points. Right: uniaxial extension ($\varepsilon_1 = \varepsilon_2 > \varepsilon_3$), where centrifugal poles and spreading points are united in a belt of solution. (b) Spherical projections of lineation fields and pitting (stippled). (c) The corresponding symmetry of the strain ellipsoid represented by a deformed cube.

scattering is compensated and the mean value of the lineation field axes shows the true symmetry of deformation.

Monoclinic and circular fields

If pure and simple shear superpose, the angle α between divergence (AD) and convergence (AC) axes, both perpendicular to AI, becomes less than 90° (Fig. 8a). AD and AC have moved symmetrically from their original positions parallel to ε_1 and ε_3. $\gamma_1 > \gamma_2$ are no longer of equal size (Figs. 6c and 8c), and the particle motions of homogenous deformation take place along distorted hyperbolas, as in Fig. 8(d) (cf. Ramberg 1975, Hoeppener *et al.* 1983, Ramsay & Huber 1983). Between AD and AC, there are two larger and two smaller parts of the lineation field (Fig. 8b). The axes of the strain ellipsoid (longitudinal strains) rotate during progressive deformation: Z approaches asymptotically towards the direction of convergence AC, but does not coincide with it; X is perpendicular to Z in every stage (Fig. 6e).

In the case of simple shear, AD and AC effectively coincide ($\alpha = 0°$) producing (Fig. 9a) a single plane of shear at 45° between ε_1 and ε_3. Z rotates towards this shear plane during progressive deformation. γ_2 has become zero (Fig. 9c) and all particle motions take place along planes parallel to γ_1 (Fig. 9d). The resulting lineation field is circular around the former AI as axis (Fig. 9d). Ferrandini & Petit (1982) and Petit *et al.* (1985) describe such lineated pebbles from the High Atlas Range; in the Molasse Basin they are rare. In conglomerates with a small mean angle α, some flat pebbles with circular fields were found with shape-planes oblique to the direction of compression, supporting an approaching of directions of compression and extension by shape-controlled field-distortion. The mean angle generally lies between 60 and 90°. Gradual transitions exist between the orthogonal uniaxial symmetries (uniaxial compression and uniaxial extension) and circular simple shear.

Triclinic symmetry

In triaxial particle motion fields the angles between all three axes can differ significantly from 90°. Common (plane) shearing, in the range between pure and simple shear, occurs by particle motions whose angle α between compressional and extensional directions varies (Fig. 10a). Further deviations from orthogonal symmetry can be analysed by introducing two other kinds of 'shearing'. If the deviation occurs between AD and AI in the plane of divergence, it is a *divergence shear* (Fig. 10b), and if the variation occurs between AI and AC in the plane of convergence, it is a *convergence shear* (Fig. 10c). Mutual superposition of two or three of them generates triclinic symmetries.

Representation of strain symmetry

Triclinic symmetries can be represented by spherical projections of the lineation field axes as points on the Schmidt net. This method is not very clear in a map with many measurements. For orthorhombic strain-fields a method similar to that for 'focal mechanism solutions' in seismology may be used (Fig. 11, middle of the back line). A sphere is cut into four quadrants along the two principal shear planes of pure shear with AI as the intersecting line. The compression quadrants, with AD in the center, are drawn black and the extension quadrants, with AC in the center, white. Superimposed simple shear can be shown by a hatched stripe on the black–white boundary in the larger angle between AD and AC, which do not persist in the centers of the quadrants (Fig. 11, middle). The black–white quadrants αremain in the position symmetrical around $\varepsilon_{1,2,3}$. The hatched stripes become proportionally larger as the angle α decreases (Fig. 11, front). For uniaxial compression (Fig. 11, back line left) a white belt of extension exists, whereas for uniaxial extension (Fig. 11, back line right) there is a black belt of compression. Belts and axes do not need to be mutually perpendicular, transitions

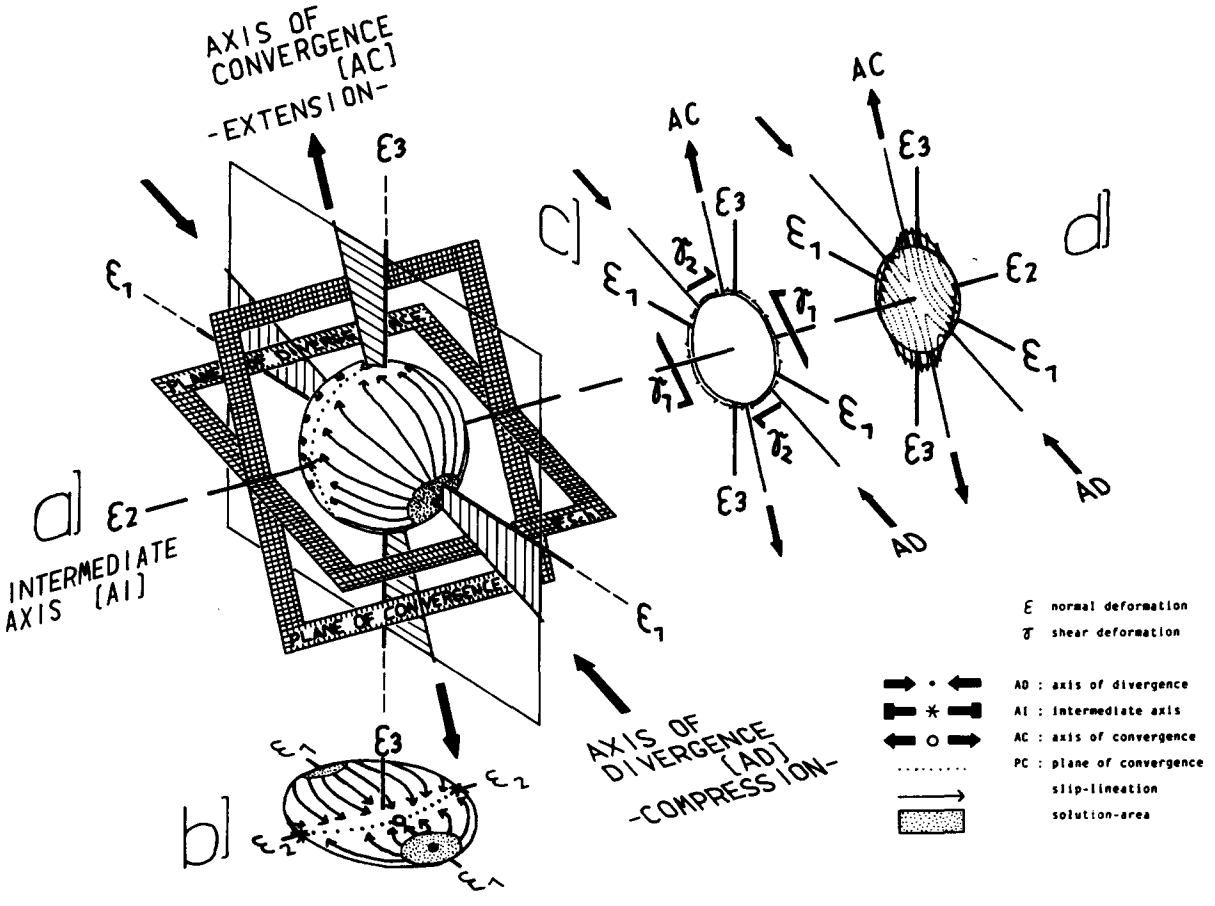

Fig. 8. Monoclinic deformation field produced by superposition of pure and simple shear. (a) Perpendicular to AI ($\triangleq \varepsilon_2$), AD and AC rotate away from ε_1 and ε_3, respectively, towards the middle (45°). (b) Between AD and AC the lineation fields are of unequal size. (c) Between ε_1 and ε_3 symmetric $\gamma_1 > \gamma_2$ are unequal and produce particle motions which are oblique hyperbolas (d).

from uniaxial cases to simple shear are also developed (Fig. 11, middle line, left and right).

Most of the Molasse pebbles examined belong in the range between pure shear, pure to simple shear with $\alpha > 60°$ and uniaxial compression.

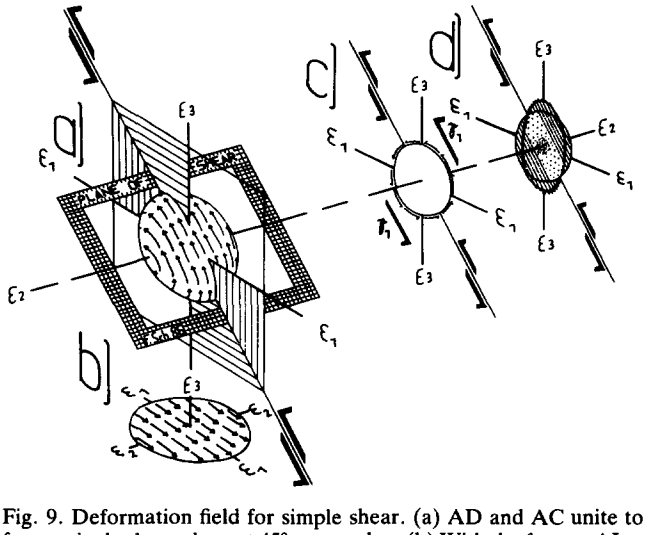

Fig. 9. Deformation field for simple shear. (a) AD and AC unite to form a single shear plane at 45° to ε_1 and ε_2. (b) With the former AI as axis the lineation field is circular and (c) only one shear-deformation γ_1 remains ($\gamma_2 = 0$), parallel to the shear plane. (d) All particle motions are parallel to γ_1.

REGIONAL RESULTS

In Fig. 1, the bedding-plane is rotated horizontally, and the lines show the horizontal projection of the direction of divergence. These imply compression perpendicular to the structures of the Alps and the eastern folded Jura (Fig. 1). The orientation is preferentially parallel to bedding, in both horizontal and folded strata. Deviations remain small and only increase towards the Alpine border. Deformed fossils (Voll 1953, Breddin 1964, Albrecht & Furtak 1965) indicate similar directions of shortening.

The Alpine Orogeny produced pebble deformation by pressure-solution in extensive areas to the north of the Alps. Deformation may have begun shortly after the deposition of the first conglomerates in the late Oligocene, but has affected even the youngest conglomerates of late Miocene age.

Regions of vertical or horizontal extension are represented by spherical projections of an orthorhombic deformation-field (Fig. 1). Since the strain symmetry is dominantly pure shear in extensive areas of the Foreland Molasse, the proportion of simple shear has not been taken into consideration in the representation. ε_3 is approximately coincident to AC. The direction of extension is mainly either vertical or horizontal. Vertical

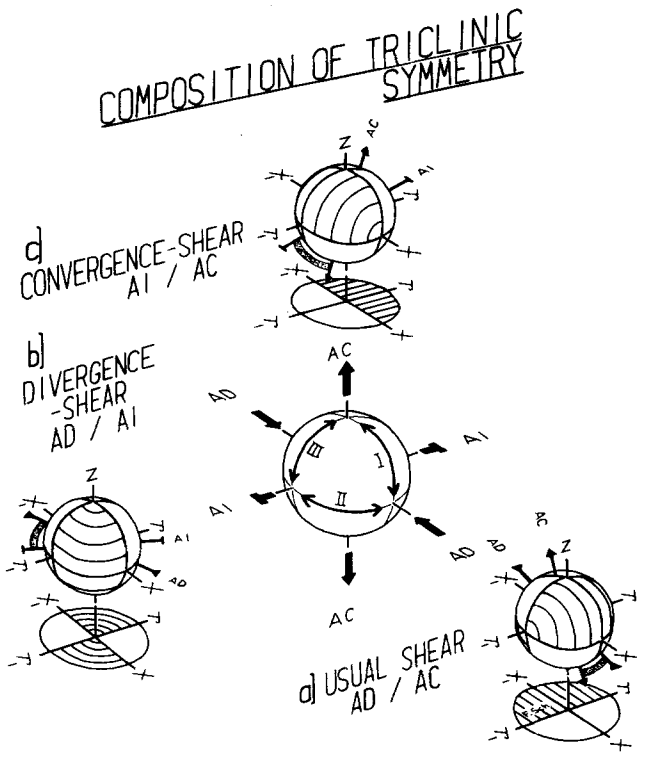

Fig. 10. Composition of triclinic symmetry. (a) Shear in the usual sense (oblique and simple shear) produces variation of the angle between AD and AC. (b) For divergent shear, the angle between AD and AI varies and (c) for convergent shear, the angle between AI and AC varies. All three deviations can occur simultaneously and superpose mutually.

extension dominates in the Subalpine Molasse, the southern Foreland Molasse and the eastern folded Jura. Horizontal extension (with a tendency towards uniaxial extension parallel to the Alpine structures) occurs in the Napf conglomerate fan and around the northern Bodensee. In the Hörnli conglomerate fan both horizontal and vertical extension can be observed at adjacent localities.

Towards the north, in the Hegau area, compression is developed perpendicular to bedding (Fig. 1); despite a thinner overburden (Lemcke 1974). AI (the horizontal component of compression) is oriented parallel to the Rhinegraben (striking NNE–SSW) and changes into compressional AD farther south. Horizontal extension parallel to the Alpine structures around the Bodensee changes into horizontal extension perpendicular to the Rhinegraben in the Hegau area. Here the conglomerates are of Tortonian age, consequently deformation must be younger. These strain axes correspond not only to the boundary structures of the Rhinegraben, but also to the stylolite systems in Suabe (Wagner 1967). Their genesis took place before the Ries-event in upper Miocene times (Wagner 1964). A present-day stress-field perpendicular to the Alpine structures can be deduced from *in situ* measurements (Greiner & Lohr 1980), or earthquakes (Ahorner 1975, Pavoni 1980, Schneider 1980). The transition from older to younger stress-field in Central Europe took place after mid-Miocene times, but not everywhere at the same time (Illies 1974). Basaltic dykes of Pliocene age in the Hegau area (Mäussnest 1973)

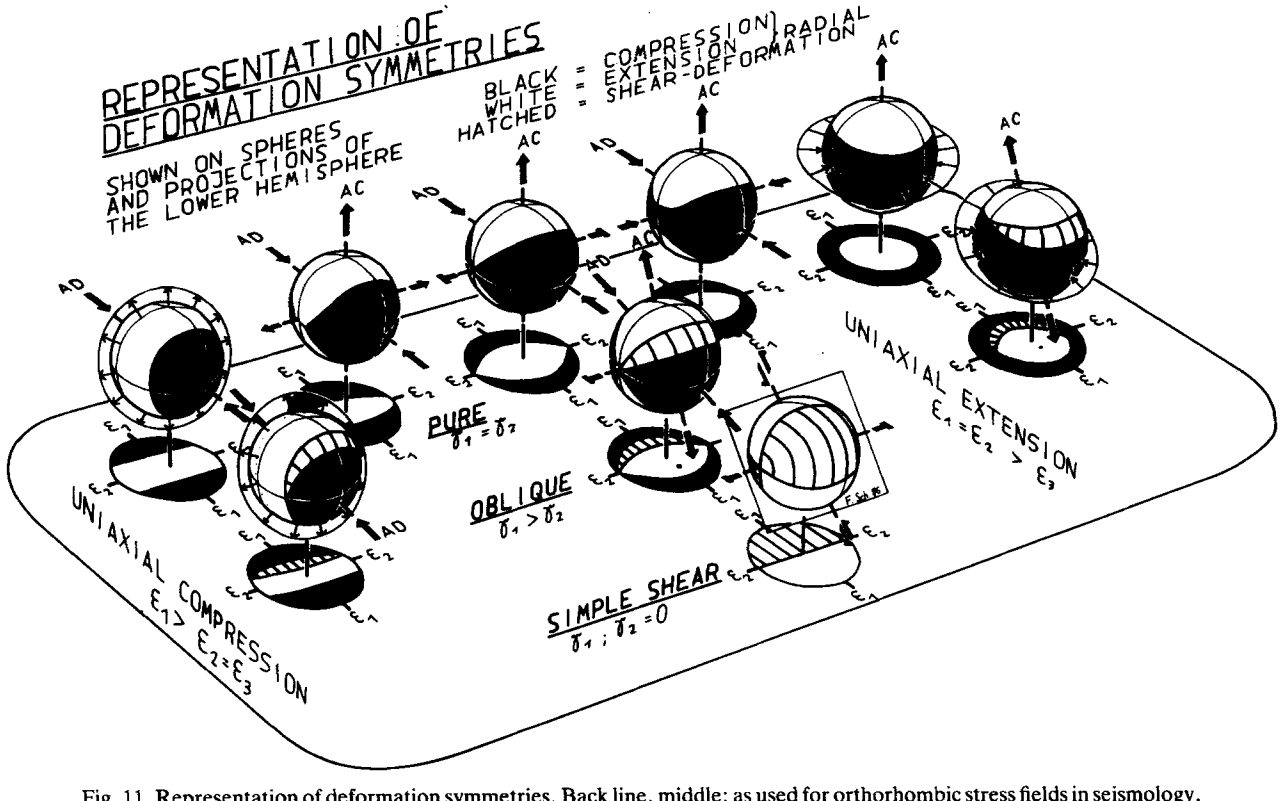

Fig. 11. Representation of deformation symmetries. Back line, middle: as used for orthorhombic stress fields in seismology, a rhombic strain field is shown by a sphere which is divided along the two principal shear planes of pure shear. The compressed quadrants with ε_1 in the center are drawn black, and the extended quadrants with ε_3 in the center are white. ε_2 is the intersecting line. Middle: superimposed simple shear can be shown by a hatched stripe in the obtuse angle between AD and AC, which are no longer in the centers of the ε-quadrants. Front: the stripe grows with the proportion of simple shear. Left corner: uniaxial compression with a white belt of extension and right corner: uniaxial extension with a black belt of compression, both of which may show transitions towards pure, simple and oblique shear.

strike nearly perpendicular to the older direction of extension. In the eastern folded Jura structures of Pliocene age (Liniger 1964) and tectonic stylolites (Plessmann 1972, Meier 1984) show a compression in a N–S direction.

Near to the Alpine border polyphase deformation-fields occur. Where bedding is tilted vertically, younger deformation-fields, with subhorizontal compression, intersect discordantly the older fields, with compression subparallel to bedding. In the centers of large conglomerate units (e.g. Pfingstboden, southwest St. Gallen) an older compression perpendicular to bedding is superposed discordantly by younger compression parallel to bedding and radial to the Alpine structures.

CONCLUSIONS

Deformational solution pits and slip-lineations on the surfaces of Molasse pebbles make visible the particle motions around the pebbles during deformation. The field of these lineations is triaxial (with directions of compression, intermediate and extension). The type of strain (pure shear, simple shear, uniaxial compression or extension and all transitions) can be seen by the mutual positions of the axes of the displacement fields. Axes and displacement paths are constant throughout the deformation process. In tectonics usually the finite deformation (strain-ellipsoid) can be seen, but there are infinite possibilities of strain paths from the original state. The displacement paths of the material moving from its original to final position around rigid pebbles can provide information about this strain path.

The amount of pebble-deformation is relatively small in the northern Alpine Molasse Basin and it is possible to record compressional and extensional directions of the early, low-grade regional deformation. The direction of compression is generally sub-parallel to bedding and arranged radial to the Alpine structures. The compressional effect of the final Alpine Orogeny on the Molasse Basin reaches far to the north where it meets the older deformational regime of southwestern Germany with the opening of the Rhinegraben.

Acknowledgements—It was the idea of Professor P. Wurster to examine the phenomenon of pebble-deformation in the Molasse Basin. I am grateful to him and Professor J. Nagel for discussions. The German Research Foundation (Deutsche Forschungsgemeinschaft) financially supported this work.

REFERENCES

Ahorner, L. 1975. Present-day stress field and seismotectonic block movements along major fault zones in Central Europe. *Tectonophysics* **29**, 233–249.

Albrecht, K. & Furtak, H. 1965. Die tektonische Verformung der Fossilien in der Faltenmolasse Oberbayerns zwischen Ammer und Leitzach. *Geol. Mitt.* **5**, 227–248.

Arthaud, F. & Mattauer, M. 1969. Exemples de stylolithes d'origine tectonique dans le Languedoc, leurs relations avec la tectonique cassante. *Bull. Soc. géol. Fr.*, 7 *ser.* **XI**, 738–744.

Behrens, M. 1977. Zur Stereometrie von Geröllen. *Mitt. geol.-paläont. Inst. Hamb.* **47**, 1–124.

Behrens, M. & Wurster, P. 1972. Tektonische Untersuchungen an Molasse-Geröllen. *Geol. Rdsch.* **61**, 1019–1037.

Blum, R. 1840. Über einige geologische Erscheinungen in der Nagelflue. *Neues Jb. Miner.* **1840**, 525–531.

Breddin, H. 1964. Die tektonische Deformation der Fossilien und Gesteine in der Molasse von St. Gallen (Schweiz). *Geol. Mitt.* **4**, 1–114.

Campredon, R., Franco, M., Giannerini, G., Gigot, P., Irr, F., Lanteaume, M., Spinni, H. & Tapoul, J.-F. 1977. Les déformations de conglomérats pliocènes de l'arc de Nice (Chaînes Subalpines méridionales). *Bull. Soc. géol. Fr.* (Suppl.) **2**, 75–77.

Estevez, A. & Sanz de Galdeano, C. 1983. Néotectonique du secteur central des chaînes Bétiques (bassins de Guadix-Baza et de Grenade). *Revue Géogr. phys. Géol. dyn.* **24**, 23–34.

Ferrandini, J. & Petit, J. P. 1982. Sur la tectonique récente de la bordure du Haut Atlas de Marrakech (Maroc). *Bull. Fac. Sci. Marrakech* **1**, 87–96.

Flinn, D. 1955. On the deformation of the Funzie conglomerate, Fetlar, Shetland. *J. Geol.* **64**, 480–505.

Füchtbauer, H. 1964. Sedimentpetrographische Untersuchungen in der älteren Molasse nördlich der Alpen. *Eclog. geol. Helv.* **57**, 157–289.

Ghosh, S. K. & Sengupta, S. 1973. Compression and simple shear of test models with rigid and deformable inclusions. *Tectonophysics* **17**, 133–175.

Greiling, R. 1985. Strukturelle und metamorphe Entwicklung an der Basis großer, weittransportierter Deckeneinheiten am Beispiel des Mittleren Allochthons in den zentralen Skandinavischen Kaledoniden (Stalon-Deckenkomplex in Västerbotten, Schweden). *Geotekt. Forsch.* **69**, 1–129.

Greiner, G. & Lohr, J. 1980. Tectonic stresses in the northern foreland of the Alpine system. *Rock Mech.* (Suppl.) **9**, 5–15.

Hancock, P. L. 1985. Brittle microtectonics: principles and practice. *J. Struct. Geol.* **7**, 437–457.

Heim, A. 1919. *Geologie der Schweiz.* I. *Molasse und Juragebirge.* Tauchnitz, Leipzig.

Hoeppener, R. 1964. Zur physikalischen Tektonik. Darstellung der affinen Deformationen, der Spannungs- und Beanspruchungszustände mit Hilfe der flächentreuen Kugelprojektion. *Felsmech. Ingenieurgeol.* **2**, 22–44.

Hoeppener, R., Brix, M. & Vollbrecht, A. 1983. Some aspects on the origin of fold-type fabrics—theory, experiments and field applications. *Geol. Rdsch.* **72**, 421–450.

Hossack, J. R. 1968. Pebble deformation and thrusting in the Bygdin area (southern Norway). *Tectonophysics* **5**, 315–339.

Illies, H. 1974. Intra-Plattentektonik in Mitteleuropa und der Rheingraben. *Oberrhein. geol. Abh.* **23**, 1–24.

Kübler, B., Pittion, J.-L., Heroux, Y., Charollais, J. & Weidmann, M. 1979. Sur le pouvoir réflecteur de la vitrinite dans quelques roches du Jura, de la Molasse et des Nappes Préalpines, Helvétiques et Penniques (Suisse occidentale et Haute-Savoie). *Eclog. geol. Helv.* **72**, 347–373.

Lemcke, K. 1974. Vertikalbewegungen des vormesozoischen Sockels im nördlichen Alpenvorland vom Perm bis zur Gegenwart. *Eclog. geol. Helv.* **67**, 121–133.

Liniger, H. 1964. Beziehungen zwischen Pliozän und Jurafaltung in der Ajoie. *Eclog. geol. Helv.* **57**, 75–90.

Lisle, R. J. 1979. Strain analysis using deformed pebbles: the influence of initial pebble shape. *Tectonophysics* **60**, 263–277.

Lohr, J. 1969. Die seismischen Geschwindigkeiten der jüngeren Molasse im ostschweizerischen und deutschen Alpenvorland. *Geophys. Prospect.* **17**, 111–125.

Mattauer, M. 1980. *Les Déformations des Matériaux de l'Écorce Terrestre.* Hermann, Paris.

Mäussnest, O. 1973. Magnetische Feldmessungen am Hauenstein bei Hornberg (Schwarzwald) und im Hohenstoffelngebiet (Hegau). *Oberrhein. geol. Abh.* **23**, 75–84.

McEwen, T. J. 1981. Brittle deformation in pitted pebble conglomerates. *J. Struct. Geol.* **3**, 25–37.

Meier, D. 1984. Zur Tektonik des Schweizer Tafel- und Faltenjuras (regionale und lokale Strukturen, Kluftgenese, Bruch- und Faltentektonik, Drucklösung). *Clausthaler Geowiss. Diss.* **14**, 1–75.

Nadai, A. 1950. *Theory of Flow and Fracture of Solids,* I. McGraw-Hill, New York.

Pavoni, N. 1980. Crustal stresses inferred from fault-plane solutions of earthquakes and neotectonic deformation in Switzerland. *Rock Mech.* (Suppl.) **9**, 63–68.

Petit, J.-P., Raynaud, S. & Cautru, J.-P. 1985. Microtectonique cassante lors du plissement d'un conglomérat (mio-pliocène du Haut Atlas–Maroc). *Bull. Soc. géol. Fr.*, 8 *ser.* **I**, 415–421.

Plessmann, W. 1972. Horizontal-Stylolithen im französisch-schweizerischen Tafel- und Faltenjura und ihre Einpassung in den regionalen Rahmen. *Geol. Rdsch.* **61**, 332–347.

Ramberg, H. 1975. Particle paths, displacement and progressive strain, applicable to rocks. *Tectonophysics* **28**, 1–37.

Ramsay, J. G. & Huber, M. I. 1983. *The Techniques of Modern Structural Geology. Vol.* 1: *Strain Analysis*. Academic Press, London.

Sander, B. 1948. *Einführung in die Gefügekunde geologischer Körper. I. Teil.* Springer, Wien.

Sanz de Galdeano, C. & Estevez, A. 1981. Estriaciones tectonicas en cantos de conglomerados. Su estudio en las depresiones de Granada y Guadix-Baza. *Estudios geol.* **37**, 227–232.

Schmidt, W. & Lindley, H. W. 1938. Scherung. *Mineralog. petrogr. Mitt.* **50**, 1–28.

Schneider, G. 1980. Seismic stresses in southern Germany. *Rock Mech.* (Suppl.) **9**, 69–73.

Schrader, F. 1987. Tektonische Deformation von Molasse-Geröllen–Erscheinung, kinematische Interpretation und regionales Gefüge. Unpublished dissertation, University of Bonn.

Teichmüller, M. & Teichmüller, R. 1975. Inkohlungsuntersuchungen in der Molasse des Voralpenlandes. *Geol. Bavar.* **73**, 123–142.

Trurnit, P. 1963. Pressure solution phenomena in detrital rocks. *Sediment. Geol.* **2**, 89–114.

Voll, G. 1953. Zur Mechanik der Molasseverformung. *Geol. Bavar.* **17**, 135–143.

Wagner, G. H. 1964. Kleintektonische Untersuchungen im Gebiet des Nördlinger Rieses. *Geol. Jb.* **81**, 519–600.

Wagner, G. H. 1967. Druckspannungsindizien in den Sedimenttafeln des Rheinischen Schildes. *Geol. Rdsch.* **56**, 906–913.